Motion Characterization for Vehicular Visible Light Communications

Khadija Ashraf, S M Towhidul Islam, Akram Sadat Hosseini, Ashwin Ashok
Georgia State University
{kashraf1,sislam9,ahosseini3}@student.gsu.edu, aashok@gsu.edu

***Abstract*—The increasing use of light emitting diodes (LED) and light receptors such as photodiodes and cameras in vehicles motivates the use of visible light communication (VLC) for inter–vehicular networking. However, the mobility of the vehicles presents a fundamental impediment for high throughput and link sustenance in vehicular VLC. While prior work has explored vehicular VLC system design, yet, there is no clear understanding on the amount of motion of vehicles in real world vehicular VLC use–case scenarios. To address this knowledge gap, in this paper, we present a mobility characterization study through extensive experiments in real world driving scenarios. We characterize motion using a constantly illuminated transmitter on a lead vehicle and a multi–camera setup on a following vehicle. The observations from our experiments reveal key insights on the degree of relative motion of a vehicle along its spatial axis and different vehicular motion behaviors. The motion characterization from this work lays a stepping stone to addressing mobility in vehicular VLC.**

I. Introduction

The extremely high bandwidth and directional nature of visible light communication (VLC) presents numerous opportunities for high throughput communication with high spatial reuse. These features make VLC an interesting case for vehicular networking using brake lights and head lights as transmitters, and optical/image sensing devices as receivers. In particular, vehicular VLC can benefit from high throughput directional links between vehicles and infrastructure (e.g. downlinks and uplinks between vehicles and road side edge/cloud computing units). The high spatial reuse factor can enable multicasting and multiple–input multiple–output (MIMO) communication (e.g. a VLC network of platooning cars, visual MIMO [1] for vehicles). However, VLC lags behind radio frequency (RF) communication in terms of adoption as a key vehicular networking technology. This is attributed to the fact that VLC links are highly directional, making them highly susceptible to throughput reduction and link failures during mobility. Therefore, realizing vehicular VLC in practice fundamentally requires addressing mobility.

Mobility is a fundamental challenge for VLC due to its line–of–sight (LOS) requirement. VLC links require strict spatial alignment between the transmitting and receiving optical elements. Such an alignment becomes extremely challenging with traditional optical receivers that use photodiodes, due to the very small cone of reception or field–of–view (FOV). The FOV in a VLC system can be increased by using a lens in front of the receiving elements, however, this makes the system noisy due to the additional collection of ambient light noise at the receiver. The noise can be spatially filtered, while maintaining a large FOV, using camera inspired receivers due to the image sensor's pixelated spatial structure. Selective filtering of ambient noise can help increase the receiver signal–to–noise ratio (SNR). The pixelated structure enables spatial resolvability (filtering) of ambient noise and the large FOV provides a larger angle of freedom for mobility for the transmitter–receiver pair. This way, camera inspired receivers present unique advantages to address the mobility issue. However, addressing the mobility problem requires a clear understanding of the amount and types of motion that the vehicular VLC system may encounter.

Prior works in vehicular VLC have largely been limited to theoretical concepts or controlled experiments in primarily static or controlled mobility settings. Only a few works in recent times have explored VLC for vehicular communication in realistic mobile settings. Shen et al [2] present their pilot studies on using a photodiode receiver and a brakelight LED transmitter for low data rate communication on real highway driving settings. The study reveals the need for a better understanding of the instantaneous motion of vehicles on the road to help *locate* the transmit beam and retain link alignment. Yamazato et al [3], conduct a motion characterization study under V2I and V2V scenarios using a LED array and a high–resolution camera. However, the experiments were conducted in a very controlled setting and did not capture the broad range of realistic vehicular movement on roadways. Additionally, the speed of the vehicle was limited to about 18-20 miles–per–hour (mph), which limits the scope of mobility characterization knowledge in context of vehicular networking.

To gain a better understanding of mobility in vehicular VLC, in this paper, we present a holistic study of the motion of the vehicles in real world driving settings. We take an approach where we make extensive measurements, using a VLC setup on real roadway driving, and derive our insights based on the observations from analyzing the measurement data sets. Our experiments involve a colored chesssboard pattern marker fixed on a lead vehicle and two (identical) cameras fixed on a following vehicle. We analyze the camera images and estimate the amount of movement of the vehicles in two spatial dimensions X and Y (see Fig. 1 (a)) in typical driving conditions. In essence, this paper presents an empirical study of motion in vehicular VLC by measuring the geometric effects on camera images, due to the relative motion between transmitter and receiver. We note that motion also leads to photometric effects such as signal quality reduction, pixel intensity reduction, motion blur etc., which we reserve for

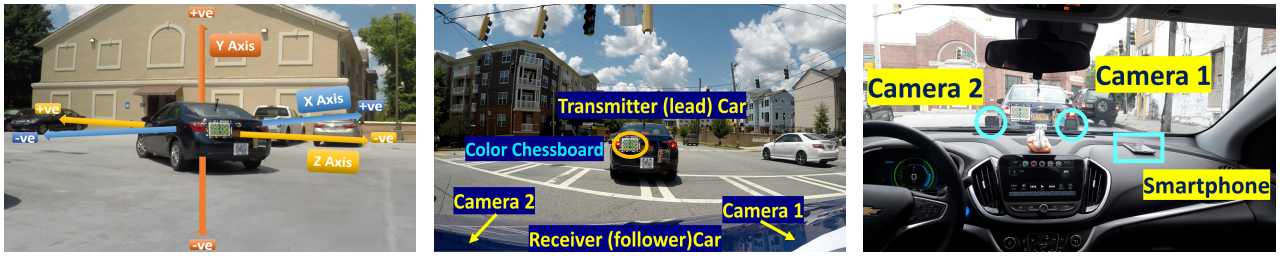

(a) Vehicle coordinate axis (b) Transmitter setup (c) Receiver setup

Fig. 1: Vehicle coordinate axis convention and experiment setup involving the lead (transmitter) and follower (receiver) vehicle

future work.

While prior work has explored mobility in vehicular VLC, to the best of our knowledge, our work presents the first extensive *study of motion of vehicles in uncontrolled real–world driving* scenarios. The data set in our study is comprehensive of about 15 hours of video footage at 30fps, which translates to analysis of over 1.5 million images (sample points).

In summary, the key contributions of this paper are as follows:

1) Definition of a motion model describing vehicle motion in 2D, measurement of vehicle motion in 2D, and a study of the relation between vehicular motion behavior (type of motion) and degree of motion through the model.
2) An extensive real–world experimentation involving multiple hours of data collection in realistic vehicular driving conditions.

II. Motion Model and Experiment Setup

We map the mobility characterization problem to the estimation of amount of motion of the vehicle in 3D space. In a wireless communication context, it is the relative motion between the transmitter and receiver that impacts the signal quality. Hence, we focus on the problem of estimating the relative motion between a transmitter vehicle and a receiver vehicle. Estimating the relative motion translates to the problem of determining the relative positioning between the two vehicles at any instance of time.

To this end, we characterize the motion of vehicles through a *motion model* that describes the relative positioning between two vehicles (transmitter and receiver) along three spatial dimensions. We define motion model as a vector,

$$\underline{M} = [\delta_u \;\; \delta_v \;\; \delta_w \;\; n] \tag{1}$$

where, δ_u captures the relative movement along horizontal (X), δ_v captures the relative movement along vertical (Y), δ_w captures the relative movement along the driving path (Z), and n is a flag value representing the vehicle behavior class type. Here, the motion model is described for a single time snapshot. The relative movement values represent the motion over a specific time window and the vehicular behavior class is the type of motion the vehicle undergoes in that specific time window. We will define and discuss the vehicle class types in detail in Section III-C.

A. Challenges in vehicular positioning

Positioning requires precise location information in 3D. Using global positioning system (GPS) coordinates of each vehicle we can determine the distance between the vehicles or the relative position of the vehicles along Z dimension. However, there is no information on the other two (X and Y) dimensions. Also, GPS is prone to errors in the typical range of 3–10 meters and upto 100 meters under poor signal reception regions. Such a degree of error, can significantly detriment the quality of a VLC link as the errors can lead to losing track of the transmitter and/or communicating with the wrong vehicle; for example, a typical lane on a highway is 4m in width and a 3m error will almost imply a different vehicle in the next lane.

Relative positioning between two vehicles on road is also extremely challenging due to the random driving behavior of the vehicles. This implies the receiver must be able to predict and/or estimate the type of transmitter vehicle motion behavior. One approach is to fit both vehicles with inertial measurement unit (IMU) sensors that can record the amount of local motion in each of 3D axis. Since the sensors are positioned on each vehicle, the transmitter will require to *inform* the receiver of the sensor value. Such a necessity creates a chicken–egg type problem, as the prime reason for exploring vehicular VLC is to establish communication between the two vehicles. While using a control radio channel to share the sensor data is a possibility, this does not scale well in realistic driving conditions. Also, IMU sensors drift with time, making them not a suitable choice for precise motion measurement.

Due to the challenges in using GPS and motion sensors, we choose to study motion in a vehicular VLC link using an optical wireless setup. In particular, we indirectly measure the amount of vehicle motion by studying the movements in the image sensor pixelated domain.

B. General Experiment Setup

The measurement study involved conducting experiments by driving two cars along different types of roads in the city of Atlanta in Georgia, USA. During the experiments it was made sure one car followed another car. Fig. 1 shows the experiment setup along with the devices placements and axis conventions used in our experimentation.

A color chessboard presenting a Bayer BGR pattern was pasted on the back of the lead car. The chessboard is treated

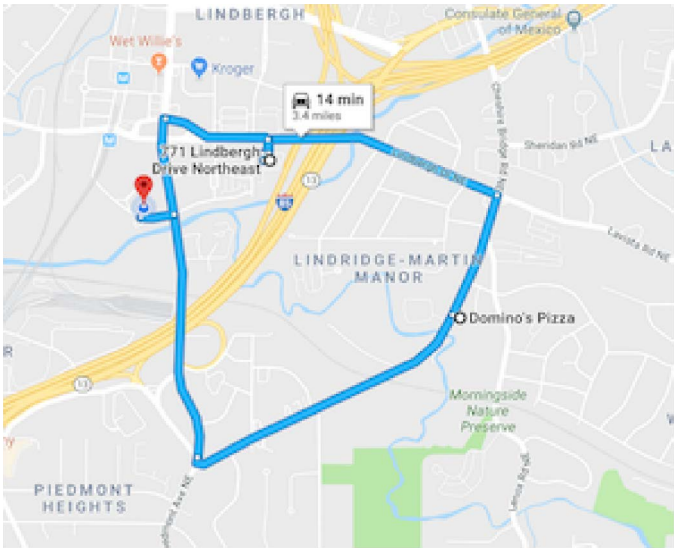

Fig. 2: Driving roadmap of experiments conducted. The picture shows the local road pathway (speeds 25–45mph). The parking lot data (speeds 5-25mph) was collected on a 30m x 100m parking lot in the location marked by the red pin on the map.

equivalent to a static–valued light transmitter. The car was followed by the receiver car that stationed two GoPro 5 HERO cameras. The two cameras were placed at a distance of 40cm along the horizontal (X) and zero relative height difference. The image view planes of the cameras were aligned parallel to one another. The camera was set to operate at 1920 x 1080 pixel resolution and at 30 fps. Unless otherwise specified, these are the default camera settings in our experiments.

The two vehicles were fit with an OBD–II diagnostic monitoring device and an Android smartphone. The OBD–II recorded the GPS coordinates (latitude and longitude) and car speed. We paired the device with an Android tablet through Bluetooth and used Torque Pro data logging application, available for download from Google Playstore. We stationed the smartphone on the car's dashboard and recorded the angular rotation along 3 axis using an inertial measurement unit (IMU) sensor logging application. We consider the rotation angles along X, Y, Z axis as pitch, azimuth and roll, respectively. The frequency of the measurements were set to 1 Hz (once per second) on both devices.

The experiments involved driving the vehicles under different road conditions and driving speeds (parking lot, local road and highway). The roadmap of the experiment driving paths is shown in Fig. 2. During the experiments the follower car drove behind the lead car, maintaining a safe driving distance. The follower car repeated the same action as the lead car. For example, if the lead car changed the lane, the follower car also changed the lane in the same direction. During this process the cameras were set to record video footage while the OBD and smartphones logged the corresponding sensor values. Overall, we collected measurements worth of about 15 hours of video and over 50000 sensor data samples. We analyze this measurement dataset to derive the motion model by using tools from computer vision, probability and statistics

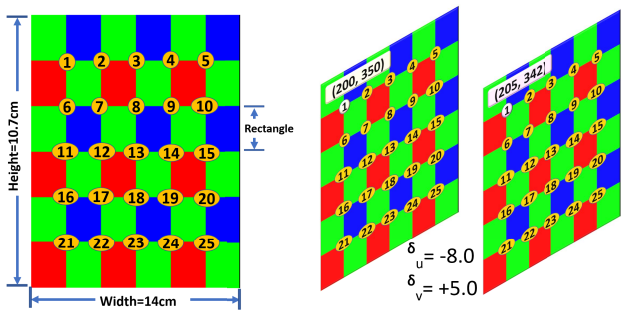

(a) Chessboard vertices (b) Sample motion computation

Fig. 3: Illustration of motion value computation using chessboard vertices. We show an example computation of δ_u and δ_v for one of the chessboard vertices.

and error analysis.

We follow a convention that, unless specified otherwise, all relative motion parameters are defined using the receiver (follower/camera) car as a reference. Therefore, every relative computation between the two cars will use *follower car value* minus *lead car value*. We assign positive (negative) polarity to motion when the lead car is to the left (right) of the camera center.

III. Horizontal and Vertical Motion

Considering the use of a camera as our measuring unit at the receiver, we denote the horizontal (X dimension: δ_u) and vertical (Y dimension: δ_v) motion parameters in *pixel* units. We consider, one pixel unit as the length corresponding to the side of one square pixel in the camera image sensor, set at the default resolution of 1920 x 1080. Given the camera intrinsic parameters (focal length and side length of a pixel and image sensor center), computed through camera calibration procedures [4], the equivalent amount of motion in world distance units (δ_u^{world}, δ_v^{world}) can be computed using perspective projection theory [5] as,

$$\Delta^{world} = \Delta^{pixels} \frac{depth}{(\frac{focal-length}{pixel-side-length})} \tag{2}$$

Here, depth is the distance between the object and camera center. In our experiments, this translates to the distance between the transmitter and receiver, equivalently the distance between the two vehicles – denoted as δ_w. This means that computation of the relative physical movement of the vehicles in X and Y dimensions requires quantifying the movement along Z dimension (estimating δ_w). From computer vision theory, a minimum of two cameras (stereo vision) setup is required to estimate depth – using stereo correspondence algorithm [6]. Depth can also be estimated from a single camera using structure from motion algorithms [6], however, that requires knowing the exact type of movement of the camera, which is technically an unknown parameter in our vehicular setup experiments. The need for depth estimation motivates the use of the two camera setup in our experimentation for vehicle motion measurements. However, due to the lack of

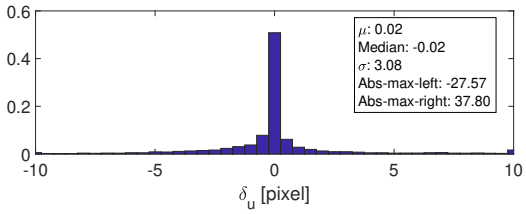

(a) δ_u 30fps

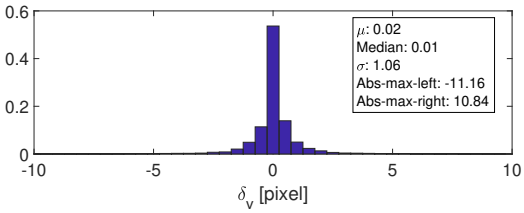

(b) δ_v 30fps

Fig. 4: Statistical representation of δ_u and δ_v in pixels at 1920 x 1080 camera resolution

(a) SW-R (b) SR (c) SW-L (d) ST

(e) LC (f) BM (g) LT (h) RT

Fig. 5: Image snapshots from our dataset that record each of the eight vehicle behavior types.
From top-left to bottom-right: sway right, straight, sway left, stop, lane change, bump,left turn, right turn.

a reliable ground–truth test bed for distance estimates (issue with some of our sensors) we reserve the motion modeling in Z (depth) for future work.

A. Measurements

We measure the horizontal and vertical motion using the pixel coordinates of the corner vertices of the imaged chessboard. Fig. 3 provides an illustration of this process. We run an open–source chessboard detection routine [7] on each image frame and record the pixel locations, (row, col), of 25 vertices (corners). We collect 25 points to provide diversity and scale the number of samples to improve the statistical estimation accuracy. If $(row_i(k), col_i(k))$ and $(row_i(k+\tau), col_i(k+\tau))$ correspond to the pixel coordinates of a vertex i (i =1,2,3..25) at time instance k and $k+\tau$, we compute the motion values as,

$$\delta_u(i,\tau) = col_i(k+\tau) - col_i(k) \quad \delta_v(i,\tau) = row_i(k+\tau) - row_i(k) \tag{3}$$

Here τ is the time period between each data (image) sample. Since we process every frame of the video, $\tau = \frac{1}{fps}$, where fps is the frame rate of the video.

B. Observations and Insights

We compute δ_u and δ_v for the entire dataset using the procedure described above, setting $fps = 30$. We also create sub–datasets by downsampling the parent dataset at lower frame rates of 1, 2 and 10fps. For 10fps we take the difference in pixel coordinates for every 3rd value in the parent dataset, and correspondingly every 15th for 2fps, and 30th for 1fps.

FPS	μ	Median	σ	Abs-max (left, right)
10-δ_u	0.03	-0.02	3.09	-26.92,37.8
2-δ_u	0.04	-0.02	3.15	-25.49, 32.61
1-δ_u	0.06	-0.02	3.16	-19.09 , 32.61
10-δ_v	0.01	0.01	1.07	-9.72 , 9.28
2-δ_v	0	0	1.02	-7.98 , 8.5
1-δ_v	-0.03	0.01	1.06	-7.98 , 6.32

TABLE I: Tabulation of the δ_u and δ_v histogram statistics.

In Fig. 4 we plot the overall probability distribution of δ_u and δ_v at 30fps frame rates. We also provide the statistical mean (μ), median, standard deviation (σ) and the maximums in each polarity. Table I summarizes the histogram statistics for 10, 2 and 1 fps camera frame rate settings.

From the histograms in Fig. 4 we can observe that δ_u is bounded within an absolute value of 40 pixels and δ_v within 12 pixels. These observations lead us to the following key insights:

(1) δ_u and δ_v range is consistent: Considering the large size of our data set, and that our measurements are across typical road driving conditions and natural driving patterns, we infer that the absolute values of δ_u and δ_v are of the range of 40 and 12 pixels, respectively. We note that these values are relative to the camera resolution of 1920 x 1080. However, translating this number to a different resolution is simple as

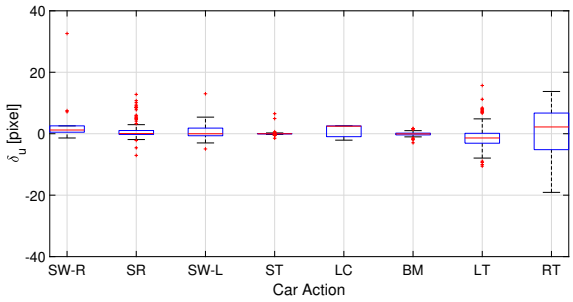

(a) δ_u, frame-rate = 30fps

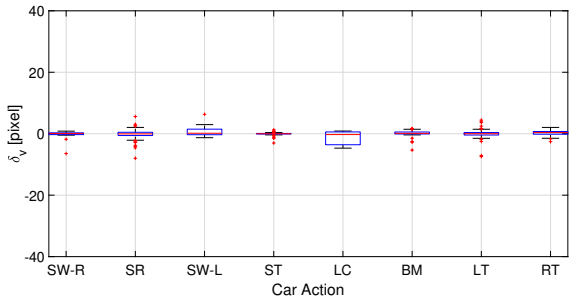

(b) δ_v, frame-rate = 30fps

Fig. 6: Horizontal and vertical motion values for different vehicle behaviors: Swaying to right inside the lane (SW-R), Straight (SR), Swaying to left inside the lane (SW-L), Stop(ST), Lane change (LC), Bumping/brake to stop (BM), Left turn (LT), Right turn (RT).

the it is a direct linear mapping (twice resolution implies 2 times the value of δ_u and δ_v) We also note that the amount of vertical movement is significantly less than the horizontal. This agrees with our general intuition that the amount of lateral movement of a vehicle would be significantly more than the vertical. However, we do also note that the vertical movement is non–zero as it must account for the vibrations of the vehicle and also jerk movements of the vehicle due to road conditions (e.g. pothole).

(2) Vehicle movement behavior impacts δ_u and δ_v: Analyzing the motion by sampling the movements at different time windows reveals that the type of motion happening in that window matters significantly. Based on the definition of the motion parameters, the value we measure corresponds to the aggregate of the motion within the sampled time window. From our measurements, we observe that the maximum movement is within 40 pixels, whether it is sampled at 30fps or 1fps. It would be wrong to generalize a theory that a longer time window sampling is a mere addition of the δ values in each sub–window. The cumulative effect over a window would be the case only when the movement of the car is continual across the accruing time windows. However, since that is not the only case in typical driving scenarios, we infer that that within any sampling time window the vehicle could be continually moving across a dimension or go back and forth (vehicle sways to left and adjusts back by swaying to the right in next window) or have a combination of multiple movements across dimensions (vehicle sways to left and turns right or stops). Depending on the length of the sampling window, the fine (intricate) movements may or may not be captured, and that only the position of the vehicle at the start and end of the window will only be registered. For example, if the vehicle moved to left in X by 10 pixels in 500ms and moved to right in X by 10pixels in next 500ms, and if the sampling rate is 1fps, the δ_u would be 0. However, this does not necessarily mean that the vehicle was relatively static. In this case, a frame rate of atleast 2fps can register the two events which will reflect as $\delta_u(k) = -10$ and $\delta_u(k+\tau) = +10$, respectively.

C. *Vehicle Movement Behavior Analysis*

We define 8 vehicle movement behavior actions and bin our data set based on the movement type through manual inspection of the videos. Each action is defined as the relative movement of the lead car with respect to the follower car. We recall that the follower car follows the same action as the lead car. As mentioned earlier, the left and right conventions are in reference to the viewing direction of the camera on the follower car. The actions (see Fig. 5) are defined as follows:

1) SW-R : vehicle sways to the right within the same lane.
2) SR : vehicle driving straight within the same lane.
3) SW-L : vehicle sways to the left within the same lane.
4) ST : vehicle is stopped within the same lane.
5) LC : vehicle is changing a lane (left or right).
6) BM : vehicle experiencing a bump and/or braking to stop.
7) LT : vehicle actively turning left.
8) RT : vehicle actively turning right.

In Fig. 6 we draw the boxplots for the measured δ_u and δ_v at each of the 8 vehicle behavior types.

On δ_u we can observe that the variance of the motion values within a particular class/type is different across the 8 classes. We observe that behaviors involving turn type movements (lane changes, active turning) have a higher variance than driving along the lane. We verify our conventions of left and right by observing that RT has a median positive value and LT has a negative median value.

On δ_v, we observe that the medians and variances are fairly uniform across the types. In general, vertical movements are more of a function of the driving path topology (driving on a hill versus flat land) than vehicle behavior.

Measuring the vertical movements across different road elevations requires further experimental investigation. However, these measurements provide a significant baseline knowledge of the range of motion along these dimensions. In addition, the variability in δ_u for different behavior types motivates deeper analysis of the temporal variance of the motion within specific time windows. We believe in further analysis of the data set can help define relevant temporal features which can be used for executing a machine learning classifier to identify and/or

predict vehicle motion behaviors. We reserve such an analysis for automatic vehicle behavior learning through motion for future work.

IV. Related Work

Vehicular VLC has been gaining increasing interest in the research community in recent times. Several works [8], [9], [10], [11], [12] have proposed techniques for improving reliability in vehicular VLC through using redundancy from LED arrays and/or using image sensors for receiver diversity. [13] proposes the use of a imaging based control channel for tracking the LED transmitter and assisting communication on a narrow FOV photodiode receiver. Such works attest to the fact that image sensors play a key role for tracking assistance and signal quality enhancement in vehicular VLC systems. Prior works on tracking LED transmitters in vehicular VLC systems have largely focused on addressing the mobility problem for niche use–cases. Such techniques have largely used a reactive approach, where the motion has affected the quality of the signal and the research aims to address the after–effects in signal quality.

Our work aims to address motion proactively, by first gaining a comprehensive understanding of the degree and type of motion in vehicular VLC systems. We will use this fundamental understanding to further develop efficient transmission and reception protocols for vehicular VLC. To this end, [14], [3] are works in recent times that have approached to modeling motion in vehicular VLC. However, the works have been largely limited to specific driving settings which impedes the generalization of such studies/models.

There is significant prior literature on the use of multiple cameras for depth estimation using stereo vision in vehicular systems [15], [16], [17]. The techniques range from using disparity images to sophisticated 3D euclidean point reconstruction. We note that our work does not claim to innovate on stereo vision algorithms. Our work presents a motivational use–case for multi–camera setups in vehicular VLC systems, and can piggyback on the advancements in stero vision depth estimation techniques.

V. Conclusion

In this paper we presented an experimental study of vehicular motion by studying the relative spatial motion using cameras. Through our experiments we generated a data set worth over 15 hours of video footage. Upon extensive analysis of our data set we inferred that the typical range of inter–frame horizontal and vertical motion of the vehicles is of the order of 40 pixels at 1920x1080 resolution at 30fps. This translates to about 25cm of lateral and vertical movement per 30ms (about 0.75meters/sec in worst case) for a typical digital video camera at 10m distance between transmitter and receiver vehicle. We also defined 8 vehicular movement behavior classes and studied the motion values for each class.

References

[1] Ashwin Ashok, Marco Gruteser, Narayan Mandayam, Jayant Silva, Michael Varga, and Kristin Dana. Challenge: Mobile optical networks through visual mimo. In *Proceedings of the Sixteenth Annual International Conference on Mobile Computing and Networking*, MobiCom '10, pages 105–112, New York, NY, USA, 2010. ACM.

[2] Wen-Hsuan Shen and Hsin-Mu Tsai. Testing vehicle-to-vehicle visible light communications in real-world driving scenarios. In *Vehicular Networking Conference (VNC), 2017 IEEE*, pages 187–194. IEEE, 2017.

[3] Takaya Yamazato, Masayuki Kinoshita, Shintaro Arai, Eisho Souke, Tomohiro Yendo, Toshiaki Fujii, Koji Kamakura, and Hiraku Okada. Vehicle motion and pixel illumination modeling for image sensor based visible light communication. *IEEE Journal on Selected Areas in Communications*, 33(9):1793–1805, 2015.

[4] Davide Scaramuzza, Agostino Martinelli, and Roland Siegwart. A toolbox for easily calibrating omnidirectional cameras. In *Intelligent Robots and Systems, 2006 IEEE/RSJ International Conference on*, pages 5695–5701. IEEE, 2006.

[5] Berthold Horn, Berthold Klaus, and Paul Horn. *Robot vision*. MIT press, 1986.

[6] Richard Hartley and Andrew Zisserman. *Multiple View Geometry in Computer Vision*. Cambridge University Press, New York, NY, USA, 2 edition, 2003.

[7] Yu Liu, Shuping Liu, Yang Cao, and Zengfu Wang. A practical algorithm for automatic chessboard corner detection. In *Image Processing (ICIP), 2014 IEEE International Conference on*, pages 3449–3453. IEEE, 2014.

[8] Bugra Turan and Seyhan Ucar. Vehicular visible light communications. In *Visible Light Communications*. InTech, 2017.

[9] Yuki Goto, Isamu Takai, Takaya Yamazato, Hiraku Okada, Toshiaki Fujii, Shoji Kawahito, Shintaro Arai, Tomohiro Yendo, and Koji Kamakura. A new automotive vlc system using optical communication image sensor. *IEEE photonics journal*, 8(3):1–17, 2016.

[10] Cen B Liu, Bahareh Sadeghi, and Edward W Knightly. Enabling vehicular visible light communication (v2lc) networks. In *Proceedings of the Eighth ACM international workshop on Vehicular inter-networking*, pages 41–50. ACM, 2011.

[11] Shintaro Arai, Yasutaka Shiraki, Takaya Yamazato, Hiraku Okada, Toshiaki Fujii, and Tomohiro Yendo. Multiple led arrays acquisition for image-sensor-based i2v-vlc using block matching. In *Consumer Communications and Networking Conference (CCNC), 2014 IEEE 11th*, pages 605–610. IEEE, 2014.

[12] Isamu Takai, Shinya Ito, Keita Yasutomi, Keiichiro Kagawa, Michinori Andoh, and Shoji Kawahito. Led and cmos image sensor based optical wireless communication system for automotive applications. *IEEE Photonics Journal*, 5(5):6801418–6801418, 2013.

[13] Tsubasa Saito, Shinichiro Haruyama, and Masao Nakagawa. A new tracking method using image sensor and photo diode for visible light road-to-vehicle communication. In *Advanced Communication Technology, 2008. ICACT 2008. 10th International Conference on*, volume 1, pages 673–678. IEEE, 2008.

[14] Masayuki Kinoshita, Takaya Yamazato, Hiraku Okada, Toshiaki Fujii, Shintaro Arai, Tomohiro Yendo, and Koji Kamakura. Motion modeling of mobile transmitter for image sensor based i2v-vlc, v2i-vlc, and v2v-vlc. In *Globecom Workshops (GC Wkshps), 2014*, pages 450–455. IEEE, 2014.

[15] Hai-Yan Zhang. Multiple moving objects detection and tracking based on optical flow in polar-log images. In *Machine Learning and Cybernetics (ICMLC), 2010 International Conference on*, volume 3, pages 1577–1582. IEEE, 2010.

[16] Taha Kowsari, Steven S Beauchemin, and Ji Cho. Real-time vehicle detection and tracking using stereo vision and multi-view adaboost. In *Intelligent Transportation Systems (ITSC), 2011 14th International IEEE Conference on*, pages 1255–1260. IEEE, 2011.

[17] Donguk Seo, Hansung Park, Kanghyun Jo, Kangik Eom, Sungmin Yang, and Taeho Kim. Omnidirectional stereo vision based vehicle detection and distance measurement for driver assistance system. In *Industrial Electronics Society, IECON 2013-39th Annual Conference of the IEEE*, pages 5507–5511. IEEE, 2013.